



## Diethylene glycol monoethyl ether-mediated nanostructured lipid carriers enhance *trans*-ferulic acid delivery by Caco-2 cells superior to solid lipid nanoparticles

HONGYU ZHANG<sup>a</sup>   
JINGWEN GUO<sup>a</sup>  
ZHI WANG  
NA WANG  
NIANPING FENG<sup>a</sup>   
YONGTAI ZHANG<sup>\*</sup>

Department of Pharmaceutical Sciences  
Shanghai University of Traditional  
Chinese Medicine, Shanghai 201203  
China

Accepted August 8, 2022  
Published online August 8, 2022

### ABSTRACT

This work aimed to compare the performance of *trans*-ferulic acid-encapsulated nanostructured lipid carriers (NLCs) and solid lipid nanoparticles (SLNs) for transport by Caco-2 cells. The NLC particles (diameter: 102.6 nm) composed of Compritol<sup>®</sup> 888 ATO, ethyl oleate, Cremophor<sup>®</sup> EL, and Transcutol<sup>®</sup> P were larger than the SLNs (diameter: 86.0 nm) formed without liquid lipid (ethyl oleate), and the former had a higher encapsulation efficiency for *trans*-ferulic acid ( $p < 0.05$ ). *In vitro* cultured Caco-2 cell transport was used to simulate intestinal absorption, and the cellular uptake of NLCs was higher than that of SLNs ( $p < 0.05$ ). Compared to SLNs, NLCs greatly enhanced *trans*-ferulic acid permeation through the Millicell<sup>™</sup> membrane ( $p < 0.05$ ). This work confirms that NLCs have better properties than SLNs in terms of increasing drug transport by Caco-2 cells. This helps to comprehend the approach by which NLC-mediated oral bioavailability of *trans*-ferulic acid is better than that mediated by SLNs, as shown in our previous report.

**Keywords:** solid lipid nanoparticles, nanostructured lipid carriers, intestinal absorption, Caco-2 cell, bioavailability

Nanocarriers are widely used in the study of oral drug delivery. They have been shown to improve the solubility of poorly water-soluble drugs and enhance drug transport across intestinal epithelial cells, thereby increasing the bioavailability of drugs (1). Solid lipid nanoparticles (SLNs) (Fig. 1) are currently the most studied drug carriers (2). SLNs generally have good biocompatibility; some can withstand autoclaving or radiation sterilization and are suitable for industrial production. However, there are also problems such as low drug-loading and encapsulation efficiency (EE) and drug leakage due to improvements in crystal order during storage (2).

<sup>a</sup> These two authors contributed to this work equally.

\* Correspondence, e-mail: analysisdrug@126.com; npfeng@shutcm.edu.cn

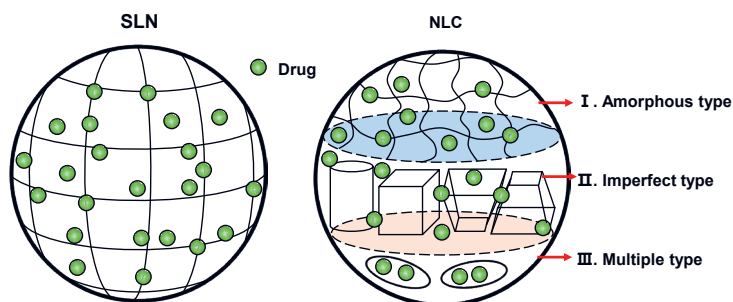


Fig. 1. Schematic of the internal structures of SLN and NLC. NLC – nanostructured lipid carrier, SLN – solid lipid nanoparticle.

Nanostructured lipid carriers (NLCs) were developed to address the deficiencies of SLNs (3). The lipid part of the NLC is formed by hybridizing solid and liquid lipid (Fig. 1). The introduction of liquid lipid destroys the original lipid arrangement of SLNs, inhibits the crystallization process, and prevents the lipid from being crystallized, thus generating more space for loading active substances (4). In addition, the presence of liquid lipids in NLCs allows active ingredients to be loaded between fatty acid chains and in the lattice defects of lipids, which increases the loading of active ingredients and reduces the probability of excretion by the crystallization of lipids during storage (5–7).

*trans*-Ferulic acid (TFA, Fig. 2a) has been shown to have potent antioxidant and anti-radiation effects; however, its oral absorption is low due to its poor solubility in water (8, 9). In our previous work, NLCs were confirmed to have superior performance for encapsulation and oral delivery of TFA than SLNs, possibly due to their increased drug solubility and enhanced intestinal cell transport (10, 11). In recent years, the Caco-2 cell model has been widely used to simulate the behavior of the human intestinal epithelium to absorb drugs. The Caco-2 cells cultured *in vitro* form a monolayer and transform into intestinal epithelial cells, which are very similar in structure and function to small intestinal epithelial cells (12), and express common characteristics like forming microvilli, brush borders, tight junctions, and other structures; secreting various enzymes including glutamine transpeptidase, alkaline phosphatase, and glucuronidase, and owning various active transporters (13). In this work, a Caco-2 cell model was established to evaluate the effect of SLNs and NLCs transported by cells and explore the potential mechanism of NLCs increasing the oral bio-availability of drugs. As strategies to accurately predict oral absorption are of tremendous importance for developing drug delivery systems, this work compared the permeability and transport capacity of SLNs and NLCs to simulate their cellular distribution, thus providing a deeper explanation of absorption differences due to microstructural differences.

## EXPERIMENTAL

### *Materials and cell lines*

Coumarin 6 (C6; Fig. 2b) was provided by Lumiprobe (USA). TFA (purity  $\geq 98\%$ ) was acquired from ZELANG Biotechnology (China). Ethyl oleate was purchased from Yunhong

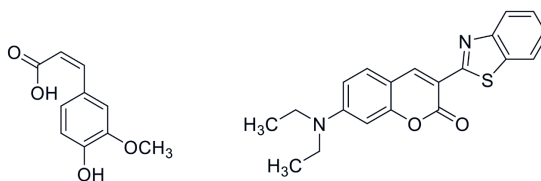


Fig. 2. Molecular structures of *trans*-ferulic acid and coumarin 6.

(China). Docosanoic acid glycerol ester (Compritol<sup>®</sup> 888 ATO) and diethylene glycol monoethyl ether (Transcutol<sup>®</sup> P) were purchased from Gattefossé (France). Polyoxyethylene castor oil (Kolliphor<sup>®</sup> EL) was from BASF (German). Dulbecco's modified Eagle medium (DMEM) and fetal bovine serum (FBS) were purchased from Gibco (USA). Caco-2 cell line was obtained from the cell bank of the Chinese Academy of Sciences (China).

#### Determination of TFA using high-performance liquid chromatography (HPLC)

TFA was quantified using LC-2010A HT HPLC (Shimadzu, Japan) with a C18 reversed-phase chromatographic column (5  $\mu\text{m}$ , 4.6 mm  $\times$  25 cm). The mobile phase consisted of methanol and 0.5 % acetic acid water in a ratio of 17:83 with a flow of 1 mL min<sup>-1</sup> and a detection wavelength of 320 nm. TFA in the range of 0.098 to 9.09  $\mu\text{g mL}^{-1}$  showed a good linear relationship with the chromatographic peak area. Samples from *in vitro* studies were centrifuged at 10,000 rpm for 10 min at 4 °C, and the TFA in the supernatant was analyzed in triplicate.

#### Preparation of TFA-loaded NLCs and SLNs

NLCs and SLNs: The formulations are shown in Table 1, and the nanoparticles were prepared using the microemulsion method (14). Briefly, lipid materials, surfactants, co-surfactants, and cargo (TFA or C6, Fig. 2) were mixed and heated to melt in a water bath at 70 °C, deionized water was added dropwise with magnetic stirring at 300 rpm, and then the hot colloidal solution was instantly placed at -20 °C for 2 h to form a uniform solid nanosuspension. The prepared NLCs and SLNs were placed at room temperature for 24 h and diluted 10-fold (V/V) with deionized water.

#### Characteristics of the prepared nanoparticles

The size distribution of the prepared lipid nanoparticles was measured at 25 °C and a diffraction angle of 90° with a dynamic light scattering method by using a Malvern Zeta-sizer Nano ZS90 Analyzer (UK).

Ultrafiltration tubes (MWCO: 10 kDa; Pall Corporation, USA) were used to separate drugs free from nanocarriers, 100  $\mu\text{L}$  of the nanodispersion was centrifuged at 11913 $\times$ g until all the dispersion medium was filtered off, and the filter cake was washed twice with 50  $\mu\text{L}$  of 50 % methanol-water solution by centrifugation (15). TFA in samples was detected by HPLC, and the detection was conducted in triplicate. The EE was calculated by equation  $EE = [(m_2 - m_1)/m_2] \times 100 \%$ , where  $m_1$  is the mass of the free drug and  $m_2$  is the total mass of the drug in the preparation.

Table I. The compositions and size distributions of TFA-loaded NLCs and candidate formulations<sup>a</sup>

Formulation	ATO (%, m/m)	EO (%, m/m)	EL (%, m/m)	TP (%, m/m)	TFA (%, m/m)	Mean diameter (nm)	EE (%)
NLCs	3.75	5.00	5.00	10.00	0.80	102.6 ± 14.3	77.3 ± 2.1
SLNs	8.75	–	5.00	10.00	0.80	86.0 ± 11.5	58.7 ± 3.3
AS	–	–	–	–	0.80	–	–

ATO, Compritol® 888 ATO; AS, aqueous solution; EE, encapsulation efficiency; EL, Kolliphor® EL; EO, ethyl oleate; NLCs, nanostructured lipid carriers; SLNs, solid lipid nanoparticles. TFA, *trans*-ferulic acid; TP, Transcutol® P.

<sup>a</sup> *n* = 3.

### Cell culture

Cells were cultured in DMEM containing 10 % FBS, 1 % non-essential amino acids, 1 % sodium pyruvate, 1 % glutamine, and 1 % cyanine streptomycin and placed in a humidified incubator with 5 % CO<sub>2</sub> at 37 °C.

### Cellular uptake

The hydrophobic fluorescent probe C6 instead of TFA was encapsulated in SLN and NLC, respectively, and the uptake of these nanoparticles by Caco-2 cells *in vitro* was compared. The Caco-2 cells were seeded into 6-well plates at a density of 50,000/cm<sup>2</sup> for 14 days, washed with phosphate buffered solution (PBS; pH 7.4) thrice, after which DMEM-diluted C6-labeled preparations were added at a different dosage of C6 (low, 1 × 10<sup>-9</sup> mol mL<sup>-1</sup>; middle, 1.9 × 10<sup>-9</sup> mol mL<sup>-1</sup>; high, 2.9 × 10<sup>-9</sup> mol mL<sup>-1</sup>), or with the same volume of fresh DMEM (blank control group, BC), cultured for 1 h; or incubated with the middle dosage for a different time. They were then washed twice with PBS, harvested with 0.25 % trypsin-0.02 % ethylene diamine tetraacetic acid (EDTA), washed with PBS thrice, and the cells were dispersed in 0.5 mL PBS. The fluorescence intensity of the samples was measured using FACS-Canto flow cytometry (Becton, Dickinson and Company, USA). Each detection was performed in triplicate.

### Transport across Caco-2 cell membranes

The Caco-2 cells were seeded onto the apical side of Millicell™ culture plate inserts (Millicell™ CPI, PCF, 0.4 μm pore size; Corning Incorporated, Corning, USA) at a density of 50,000/cm<sup>2</sup> and cultured for about 3 weeks until the resistance across the monolayers value (Trans Epithelial Electric Resistance, TEER) was ≥ 600 Ω cm<sup>2</sup>. Next, cells were washed twice and incubated with Hank's solution (pH 7.4) for 30 min; then, 0.4 mL of Hank's solution containing the tested preparation and 0.6 mL of fresh Hank's solution, respectively, were added to the apical and basolateral sides. A 100 μL sample was removed from the basolateral side at a predetermined time, while the remainder of the solution was supplemented with an equal volume of fresh Hank's solution preheated to 37 °C. TFA in samples was detected by HPLC, and each determination was performed in triplicate.

### Statistical analysis

Data are expressed as mean  $\pm$  SD. SPSS 17.0 (SPSS, Chicago, USA) was used for the statistical analyses. Statistical calculation was performed using a one-way ANOVA test, with  $p < 0.05$  considered statistically significant.

## RESULTS AND DISCUSSION

### Characteristics of the prepared nanoparticles

We prepared lipid nanoparticles by the microemulsion method as this process does not require organic solvents and special equipment such as high shear machines and high-pressure homogenizers (16, 17). This low-energy and green preparation method is conducive to industrialization.

Long-chain fatty acids and long-chain triglycerides have been reported to produce larger particle sizes than medium-chain fatty acids and medium-chain triglycerides, possibly due to the fluidity of internal lipids and the surfactant layer increased (18). Additionally, long-chain lipid-based NLCs are absorbed through the intestinal lymphatic system with enhanced bioavailability and prolonged half-life (19). In this work, we used Compritol® 888 ATO and ethyl oleate with long-chains as the oil phase so that the resulting nano-carriers with relatively large particle size and thus have a larger internal lipid space to load more drugs, as well as achieving uptake by the intestinal lymphatic system (20). With the addition of liquid lipid, the mean size of the NLC was significantly larger than that of the SLN formed only by the solid lipid in the lipid core (Table 1). Additionally, the NLC with lower crystallinity and greater space provided by liquid lipid achieved higher EE for TFA than SLN ( $p < 0.01$ ).

Preliminary experiments show that TFA can be dissolved in ethyl oleate, which ensures that the drug is preferentially dissolved in the lipid core during the preparation process and have good physicochemical stability (21). After 60 days of storage at room temperature, the particle size distribution of the NLCs and SLNs did not change significantly (Fig. 3).

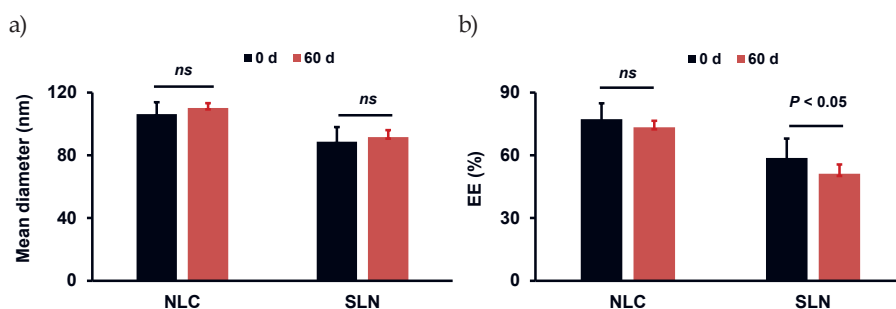


Fig. 3. a) Size distribution and b) EE of *trans*-ferulic acid-loaded NLC and SLN stored at room temperature for 60 days ( $n = 3$ ). EE – encapsulation efficiency, NLC – nanostructured lipid carrier, SLN – solid lipid nanoparticle.

However, the EE of SLN decreased significantly ( $p < 0.05$ ), suggesting drug leakage during prolonged storage, while the NLC reduced drug expulsion due to its low crystallinity or disordered lipid core.

### Cellular uptake

Studies have shown that cell absorption of particle drug delivery systems such as SLNs occurs mainly through the paracellular pathway, cell phagocytosis, receptor-mediated endocytosis, and other pathways (22). The interaction of nanocarriers with cells, including their transcellular behavior, is crucial for the design of oral drug delivery systems as well as for the safety studies of potential nanomaterials. However, tracking these systems inside cells requires complex probe tagging strategies. Fluorescence probes such as C6 monitor nanoparticle migration through intestine tissues and help determine accumulation sites, thus providing a better understanding of nanostructures. As its excellent laser conversion rate and high detection sensitivity, C6 was a powerful tool used to quantify and visualize nanoparticle accumulation in cells and tissues. The fluorescence intensity of the cells represents the cellular uptake of the nanoparticles. Regardless of whether they were incubated for 15 min or 60 min, the fluorescence intensity of cells in the SLN group was higher ( $p < 0.01$ ) than that of the NLC group, suggesting that the uptake of SLNs by cells was significantly greater than that of NLCs (Fig. 4). The easily quenched fluorophore of C6 in water may lead to the fluorescence intensity of cells in SLN and NLC groups decreasing with the prolongation of incubation time. In addition, the smaller particle size and faster drug release resulted in a stronger fluorescence intensity of C6 taken up into cells from SLNs than from NLCs (23).

Furthermore, the fluorescence intensity of each dose group of SLN was higher ( $p < 0.01$ ) than that of the NLC group (Fig. 5). However, with the dose increase, the fluorescence intensity of SLN and NLC groups showed a weakening trend. We speculate that this is related to the high concentration of nanoparticles in the culture medium. NLCs are generally considered safe, but the emulsifiers in the nanoparticle components and the fatty acids produced by lipid degradation by cells may inhibit the physiological activity of cells at

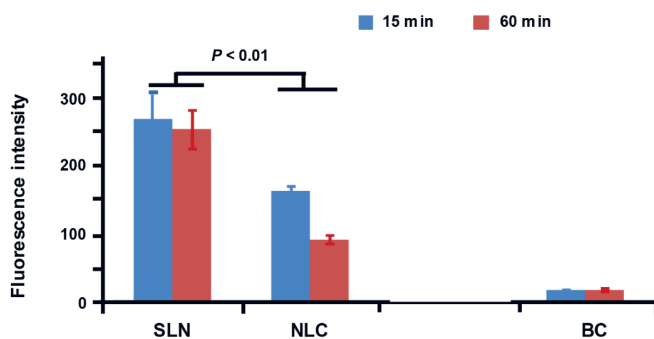


Fig. 4. Fluorescence intensity of Caco-2 cells incubated with the same dosage of coumarin 6-labeled NLC and SLN for a different time ( $n = 3$ ). BC – blank control, NLC – nanostructured lipid carrier, SLN – solid lipid nanoparticle.

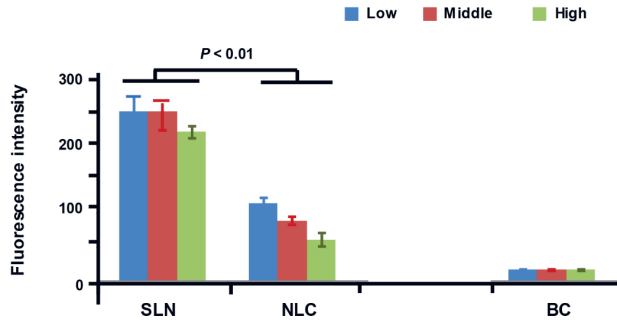


Fig. 5. The fluorescence intensity of Caco-2 cells incubated with different coumarin 6-labeled NLC and SLN with a low, middle, and high dosage of C6 ( $n = 3$ ). BC – blank control, NLC – nanostructured lipid carrier, SLN – solid lipid nanoparticle.

high concentrations (24–26). It has been reported that  $2.1 \times 10^{11}$  particles/mL decreased lymphocyte viability to 55 % (27). Given that the gastrointestinal physiological environment is quite different from in vitro cell models, coupled with dose control, more work needs to be done to assess the safety of NLCs.

#### Transport capacity across Caco-2 cell membrane

For poorly soluble drugs, increasing solubility is considered an effective way to improve bioavailability, especially for class II (*e.g.*, raloxifene) and class IV (*e.g.*, saquinavir) drugs (28, 29). The liquid lipid in the lipid core enhances the encapsulation performance of NLC for poorly soluble TFA, which is stronger than that of SLN, thus obtaining greater solubility and facilitating the intestinal absorption of drugs. The cumulative drug permeation from TFA-loaded nanocarriers across the Caco-2 cell monolayer on the PCF membrane

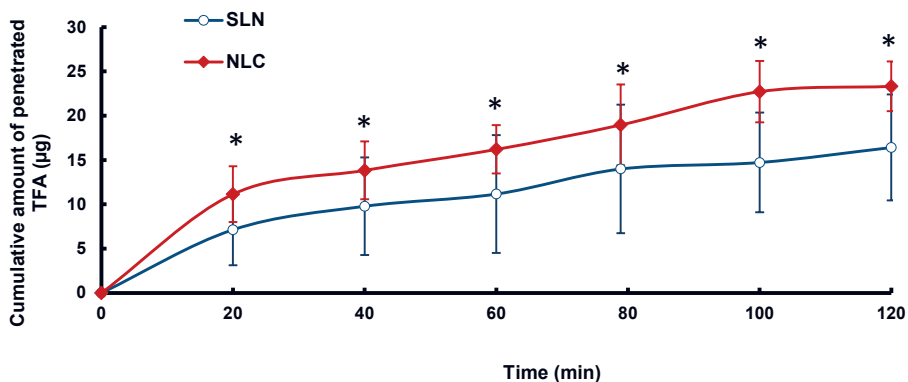


Fig. 6. Cumulative drug permeation from TFA-loaded nanocarriers across Caco-2 cell monolayer membrane (SLN group compared with NLC group,  $* p < 0.05$ ,  $n = 3$ ). NLC – nanostructured lipid carrier, SLN – solid lipid nanoparticle, TFA – *trans*-ferulic acid.

in Millicell™ is shown in Fig. 6. TFA delivered by NLC across the Caco-2 cell monolayer was more efficient than SLN at each time point ( $p < 0.05$ ), indicating that NLC was conducive to drug transmembrane transport and superior to SLN. Since the nanocarriers-mediated drug transport across Caco-2 cell monolayer has both paracellular and transcellular pathways. The current results showed that the transcellular transport efficiency of NLC is lower than that of SLN. Thus paracellular transport of NLC should be stronger than that of SLN.

The NLC is hybridized by liquid lipid and with more softness enhanced accessing the intercellular space. The surfactants (Kolliphor® EL and Transcutol® P) from the carriers act as a permeability enhancer to temporarily open tight intercellular junctions, resulting in higher drug delivery through the intestinal epithelial cell layer (Fig. 7) (30). The additional liquid lipid in NLC can be digested into more micelles by digestive enzymes than SLN, contributing to the delivery of the drug through the cell layer. Previous reports indicate that in the *in vivo* environment, these micelles, together with drugs, are absorbed by

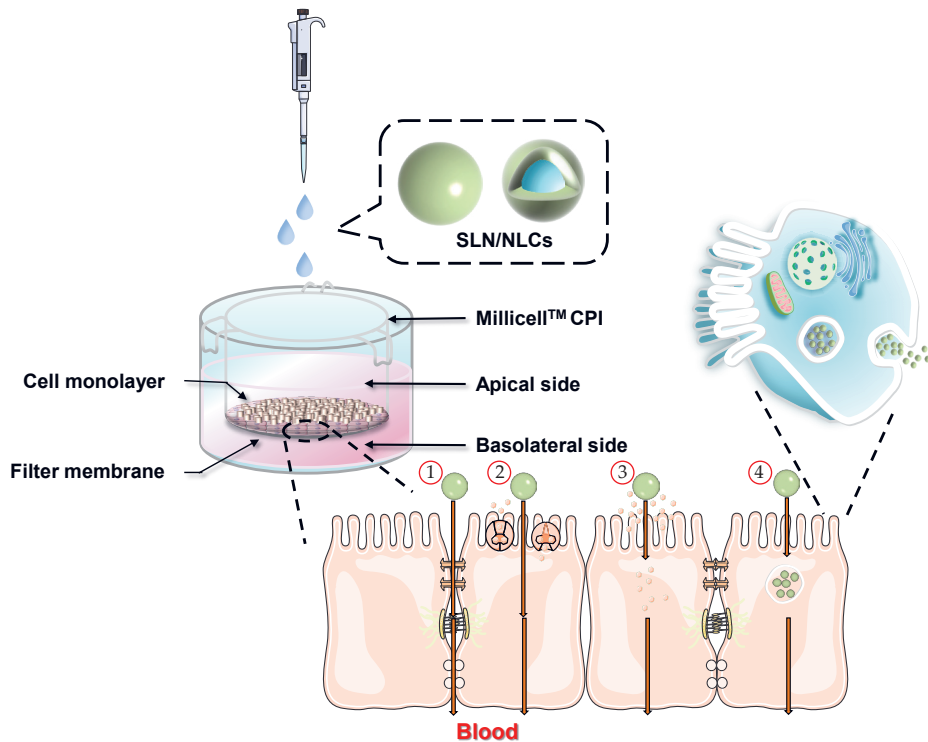


Fig. 7. Schematic diagram of Millicell™ CPI cultured Caco-2 cell monolayer mimicking intestinal epithelial cells for evaluating NLC and SLN for oral drug delivery. The nanocarriers-mediated drug transport across Caco-2 cell monolayer includes (1) paracellular, (2) transportation mediated by proteins, (3) passive diffusion after drug release, and (4) transcellular pathways. NLC – nanostructured lipid carrier, SLN – solid lipid nanoparticle.



intestinal epithelial cells, re-esterified through the monoacylglycerol or phosphatidic acid pathway, and converted into chylomicrons are absorbed into the lymphatic vessels, enhancing drug absorption (31–32).

## CONCLUSIONS

The present results show that NLCs have stronger drug-loading properties and more efficient delivery of TFA across the simulated intestinal epithelial cell layer *in vitro* as compared to SLNs, thus providing a possible mechanism for the former to enhance the oral bioavailability of TFA. However, more in-depth studies, including the mechanism of uptake by Caco-2 cells, the behavior of nanoparticles across the intestinal mucus layer, and the role of M cells, are of great significance for elucidating the mechanism of intestinal absorption of NLC.

*Declaration of interests.* – The authors declare no conflicts of interest.

*Funding.* – The authors are very grateful for the financial support. This work was financially supported by the National Natural Science Foundation of China (81673612), the Program for Professor of Special Appointment (Eastern Scholar) at Shanghai Institutions of Higher Learning (TP2020054), and the National training program for innovative talents of Traditional Chinese Medicine (T20194828003).

*Author's contributions.* – Conceptualization, Y. Z. and N. F.; methodology, H. Z., J. G., and N. W.; analysis, H. Z., J. G., and Z. W.; investigation, Y. Z. and N. F.; writing, original draft preparation, J. G.; writing, review and editing, Y. Z. All authors have read and agreed to the published version of the manuscript.

## REFERENCES

1. Y. Liu, Z. Jiang, X. Hou, X. Xie, J. Shi, J. Shen, Y. He, Z. Wang and N. Feng, Functional lipid polymeric nanoparticles for oral drug delivery: Rapid mucus penetration and improved cell entry and cellular transport, *Nanomedicine* **21** (2019) Article ID 102075; <https://doi.org/10.1016/j.nano.2019.102075>
2. J. Akbari, M. Saeedi, F. Ahmadi, S. M. H. Hashemi, A. Babaei, S. Yaddollahi, S. S. Rostamkalaei, K. Asare-Addo and A. Nokhodchi, Solid lipid nanoparticles and nanostructured lipid carriers: A review of the methods of manufacture and routes of administration, *Pharm Dev. Technol.* **27**(5) (2022) 525–544; <https://doi.org/10.1080/10837450.2022.2084554>
3. Y. R. Neupane, M. D. Sabir, N. Ahmad, M. Ali and K. Kohli, Lipid drug conjugate nanoparticle as a novel lipid nanocarrier for the oral delivery of decitabine: ex vivo gut permeation studies, *Nanotechnology* **24**(41) (2013) Article ID 415102; <https://doi.org/10.1088/0957-4484/24/41/415102>
4. Q. Xia, A. Saupe, R. H. Müller and E. B. Souto, Nanostructured lipid carriers as novel carrier for sunscreen formulations, *Int. J. Cosmet. Sci.* **29**(6) (2007) 473–482; <https://doi.org/10.1111/j.1468-2494.2007.00410.x>
5. R. Augustine, A. A. Mamun, A. Hasan, S. A. Salam, R. Chandrasekaran, R. Ahmed and A. S. Thakor, Imaging cancer cells with nanostructures: Prospects of nanotechnology driven non-invasive cancer diagnosis, *Adv. Colloid Interface Sci.* **294** (2021) Article ID 102457; <https://doi.org/10.1016/j.cis.2021.102457>
6. H. Liu, Z. Cai, F. Wang, L. Hong, L. Deng, J. Zhong, Z. Wang and W. Cui, Colon-targeted adhesive hydrogel microsphere for regulation of gut immunity and flora, *Adv. Sci. (Weinheim)* **8**(18) (2021) e2101619 (12 pages); <https://doi.org/10.1002/advs.202101619>
7. X. Zheng, C. Qiu, J. Long, A. Jiao, X. Xu, Z. Jin and J. Wang, Preparation and characterization of porous starch/ $\beta$ -cyclodextrin microsphere for loading curcumin: Equilibrium, kinetics and mechanism of adsorption, *Food Biosci.* **41** (2021) Article ID 101081; <https://doi.org/10.1016/j.fbio.2021.101081>

8. M. Fröhbauerová, L. Červenka, T. Hájek, M. Pouzar and J. Palarčík, Bioaccessibility of phenolics from carob (*Ceratonia siliqua* L.) pod powder prepared by cryogenic and vibratory grinding, *Food Chem.* **377** (2022) Article ID 131968; <https://doi.org/10.1016/j.foodchem.2021.131968>
9. T. Peng, Y. Wang, T. Yang, F. Wang, J. Luo and Y. Zhang, Physiological and biochemical responses, and comparative transcriptome profiling of two *Angelica sinensis* cultivars under enhanced ultraviolet-B radiation, *Front Plant. Sci.* **12** (2021) Article ID 805407 (18 pages); <https://doi.org/10.3389/fpls.2021.805407>
10. Y. Zhang, Z. Li, K. Zhang, G. Yang, Z. Wang, J. Zhao, R. Hu and N. Feng, Ethyl oleate-containing nanostructured lipid carriers improve oral bioavailability of *trans*-ferulic acid as compared with conventional solid lipid nanoparticles, *Int. J. Pharm.* **511**(1) (2016) 57–64; <https://doi.org/10.1016/j.ijpharm.2016.06.131>
11. R. F. S. Gonçalves, J. T. Martins, L. Abrunhosa, J. Baixinho, A. A. Matias, A. A. Vicente and A. C. Pinheiro, Lipid-based nanostructures as a strategy to enhance curcumin bioaccessibility: Behavior under digestion and cytotoxicity assessment, *Food Res. Int.* **143** (2021) Article ID 110278; <https://doi.org/10.1016/j.foodres.2021.110278>
12. E. T. Rodrigues, S. F. Nascimento, C. L. Pires, L. P. Godinho, C. Churro, M. J. Moreno and M. A. Pardal, Determination of intestinal absorption of the paralytic shellfish toxin GTX-5 using the Caco-2 human cell model, *Environ. Sci. Pollut. Res. Int.* **28**(47) (2021) 67256–67266; <https://doi.org/10.1007/s11356-021-15342-y>
13. S. Youhanna and V. M. Lauschke, The past, present and future of intestinal in vitro cell systems for drug absorption studies, *J. Pharm. Sci.* **110**(1) (2021) 50–65; <https://doi.org/10.1016/j.xphs.2020.07.001>
14. R. Hu, S. Liu, G. Anwaier, Q. Wang, W. Shen, Q. Shen and R. Qi, Formulation and intestinal absorption of naringenin loaded nanostructured lipid carrier and its inhibitory effects on nonalcoholic fatty liver disease, *Nanomedicine* **32** (2021) Article ID 102310; <https://doi.org/10.1016/j.nano.2020.102310>
15. Q. Yu, X. Hu, Y. Ma, Y. Xie, Y. Lu, J. Qi, L. Xiang, F. Li and W. Wu, Lipids-based nanostructured lipid carriers (NLCs) for improved oral bioavailability of sirolimus, *Drug Deliv.* **23**(4) (2016) 1469–1475; <https://doi.org/10.3109/10717544.2016.1153744>
16. J. Akbari, M. Saeedi, F. Ahmadi, S. Hashemi, A. Babaei, S. Yaddollahi, S. S. Rostamkalaei, K. Asare-Addo and A. Nokhodchi, Solid lipid nanoparticles and nanostructured lipid carriers: A review of the methods of manufacture and routes of administration, *Pharm. Dev. Technol.* **27**(5) (2022) 525–544; <https://doi.org/10.1080/10837450.2022.2084554>
17. Z. Cheng, Y. Li, K. Wang, X. Zhu, P. Tharkar, W. Shu, T. Zhang, S. Zeng, L. Zhu, M. Murray, W. Czranowski and F. Zhou, Compritol solid lipid nanoparticle formulations enhance the protective effect of betulinic acid derivatives in human Müller cells against oxidative injury, *Exp. Eye Res.* **215** (2022) Article ID 108906; <https://doi.org/10.1016/j.exer.2021.108906>
18. V. Pokharkar, A. Patil-Gadhe and G. Kaur, Physicochemical and pharmacokinetic evaluation of rosuvastatin loaded nanostructured lipid carriers: influence of long- and medium-chain fatty acid mixture, *J. Pharm. Investig.* **48** (2018) 465–476; <https://doi.org/10.1007/s40005-017-0342-8>
19. H. Shete, S. Chatterjee, A. De and V. Patravale, Long chain lipid based tamoxifen NLC. Part II: pharmacokinetic, biodistribution and in vitro anticancer efficacy studies, *Int. J. Pharm.* **454**(1) (2013) 584–592; <https://doi.org/10.1016/j.ijpharm.2013.03.036>
20. P. Ganesan, P. Ramalingam, G. Karthivashan, Y. T. Ko and D. K. Choi, Recent developments in solid lipid nanoparticle and surface-modified solid lipid nanoparticle delivery systems for oral delivery of phyto-bioactive compounds in various chronic diseases, *Int. J. Nanomedicine* **13** (2018) 1569–1583; <https://doi.org/10.2147/IJN.S155593>
21. M. Elmowafy, K. Shalaby, H. M. Ali, N. K. Alruwaili, A. Salama, M. F. Ibrahim, M. A. Akl and T. A. Ahmed, Impact of nanostructured lipid carriers on dapsone delivery to the skin: in vitro and in vivo studies, *Int. J. Pharm.* **572** (2019) Article ID 118781; <https://doi.org/10.1016/j.ijpharm.2019.118781>
22. S. Haddadzadegan, F. Dorkoosh and A. Bernkop-Schnürch, Oral delivery of therapeutic peptides and proteins: Technology landscape of lipid-based nanocarriers, *Adv. Drug Deliv. Rev.* **182** (2022) Article ID 114097 (26 pages); <https://doi.org/10.1016/j.addr.2021.114097>

23. Y. Zhang, Z. Li, K. Zhang, G. Yang, Z. Wang, J. Zhao, R. Hu and N. Feng, Ethyl oleate-containing nanostructured lipid carriers improve oral bioavailability of *trans*-ferulic acid as compared with conventional solid lipid nanoparticles, *Int. J. Pharm.* **511**(1) (2016) 57–64; <https://doi.org/10.1016/j.ijpharm.2016.06.131>
24. L. Zhou, Y. Chen, Z. Zhang, J. He, M. Du and Q. Wu, Preparation of tripterine nanostructured lipid carriers and their absorption in rat intestine, *Pharmazie* **67**(4) (2012) 304–310; <https://doi.org/10.1691/ph.2012.1108>
25. H. S. Rahman, A. Rasedee, H. H. Othman, M. S. Chartrand, F. Namvar, S. K. Yeap, N. Abdul Samad, R. J. Andas, N. Muhammad Nadzri, T. Anasamy, K. B. Ng and C. W. How, Acute toxicity study of zerumbone-loaded nanostructured lipid carrier on BALB/c mice model, *Biomed. Res. Int.* **2014** (2014) Article ID 563930 (15 pages); <https://doi.org/10.1155/2014/563930>
26. J. Y. Fang, C. L. Fang, C. H. Liu and Y. H. Su, Lipid nanoparticles as vehicles for topical psoralen delivery: solid lipid nanoparticles (SLN) versus nanostructured lipid carriers (NLC), *Eur. J. Pharm. Biopharm.* **70**(2) (2008) 633–640; <https://doi.org/10.1016/j.ejpb.2008.05.008>
27. L. P. Mendes, J. M. F. Delgado, A. D. A. Costa, M. S. Vieira, P. L. Benfica, E. M. Lima and M. C. Valadares, Biodegradable nanoparticles designed for drug delivery: the number of nanoparticles impacts on cytotoxicity, *Toxicol. in Vitro* **29**(6) (2015) 1268–1274; <https://doi.org/10.1016/j.tiv.2014.12.021>
28. N. V. Shah, A. K. Seth, R. Balaraman, C. J. Aundhia, R. A. Maheshwari and G. R. Parmar, Nanostructured lipid carriers for oral bioavailability enhancement of raloxifene: Design and in vivo study, *J. Adv. Res.* **7**(3) (2016) 423–434; <https://doi.org/10.1016/j.jare.2016.03.002>
29. A. Beloqui, M. Á. Solinís, A. R. Gascón, A. del Pozo-Rodríguez, A. des Rieux and V. Prétat, Mechanism of transport of saquinavir-loaded nanostructured lipid carriers across the intestinal barrier, *J. Control. Release* **166**(2) (2013) 115–123; <https://doi.org/10.1016/j.jconrel.2012.12.021>
30. A. Ali Khan, J. Mudassir, N. Mohtar and Y. Darwis, Advanced drug delivery to the lymphatic system: lipid-based nanoformulations, *Int. J. Nanomedicine* **8**(1) (2013) 2733–2744; <https://doi.org/10.2147/IJN.S41521>
31. X. Zhou, X. Zhang, Y. Ye, T. Zhang, H. Wang, Z. Ma and B. Wu, Nanostructured lipid carriers used for oral delivery of oridonin: an effect of ligand modification on absorption, *Int. J. Pharm.* **479**(2) (2015) 391–398; <https://doi.org/10.1016/j.ijpharm.2014.12.068>
32. R. Ghadi and N. Dand, BCS class IV drugs: Highly notorious candidates for formulation development, *J. Control. Release* **248** (2017) 71–95; <https://doi.org/10.1016/j.jconrel.2017.01.014>
33. V. Makwana, R. Jain, K. Patel, M. Nivsarkar and A. Joshi, Solid lipid nanoparticles (SLN) of efavirenz as lymph targeting drug delivery system: Elucidation of mechanism of uptake using chylomicron flow blocking approach, *Int. J. Pharm.* **495**(1) (2015) 439–446; <https://doi.org/10.1016/j.ijpharm.2015.09.014>